2008 IEEE International Conference on
Robotics and Automation
Pasadena, CA, USA, May 19-23, 2008

On Iterative Learning Control for Simultaneous Force/Position Trajectory Tracking by using a 5 D.O.F. Robotic Thumb under Non-Holonomic Rolling Constraints

Kenji Tahara, Suguru Arimoto, Masahiro Sekimoto, Morio Yoshida and Zhi-Wei Luo

Abstract— **This paper proposes an iterative learning control method for simultaneous force/position tracking tasks by using a 5 D.O.F. robotic thumb under non-holonomic rolling constraints. In our previous works, "blind touching", which is defined as a point-to-point control scheme for the robot to realize a desired contact position and a contact force simultaneously without any external sensing, have proposed. In this paper, an iterative learning control manner to realize a desired continuous trajectory of the center of the contact point together with a desired contact force on the task plane is proposed. The usefulness of this learning control method is demonstrated by showing results of computer simulations.**

I. INTRODUCTION

It is well-known that in order for a robotic manipulator to realize a desired trajectory tracking, the iterative learning control is one of the effective control methods because it does not need the accurate model information of the system.

Until now, many researches concerned with the learning control method have been reported [1–8]. Uchiyama [1] firstly proposed a naive idea of iterative learning control, and Arimoto *et al.* firstly proved the convergence of trajectory tracking analytically by showing a sufficient condition of D-type learning [2]. After that, Arimoto *et al.* have extended this method to PI-type learning control and hybrid force and position trajectory tracking control in the case that there exists a holonomic constraint between the end-effector of the manpulator and a task plane by using non-redundant robot manipulators [3–5]. Most of researches in the case of a redundant system have basically proposed learning control update laws in joint space except for De Luca's works [6], [7] which employed a frequence-domain learning method. Very resently, Arimoto *et al.* have proposed a generic iterative learning control scheme for redundant joint systems based on learning updates only in task space, and also have extended to the case of existence of a holonomic constraint between the end effector of the manipulator and a task plane [9]. On the other hand, Fujimoto *et al.* have proposed an iterative learning control for a certain class of Hamiltonian systems with non-holonomic constraints in order to solve optimal control problems by using the symmetric property of Hamiltonian systems, and showed the usefulness of this controller via numerical simulation of a rolling coin and vehicle system [10], [11].

On the other hand, in our previous work, we have proposed "blind touching" by using a 5 D.O.F. robotic thumb model with soft and deformable hemispherical finger-tip [12]. The "blind touching" is defined in this research as a hybrid contact position and force control method, that can construct control signals on the basis of only kinematic informations of the robotic thumb itself and measurable state variables obtained by internal sensors (joint angles and angular velocities), and does not need any external sensing such as vision, force or tactile sensing. However, we have only treated a point-to-point control, and not yet considered a desired continuous trajectory tracking control.

In this paper, we extend "blind touching" to simultaneous force/position tracking tasks according to the iterative learning control manner by using a 5 D.O.F. robotic thumb under non-holonomic rolling constraints to realize a desired trajectory of the center of the contact area together with fulfilling a desired contact force. Firstly, the 5 D.O.F. robotic thumb with soft and deformable hemispherical finger-tip through taking into consideration the 3-Dimensional non-holonomic rolling constraints are modeled. In this modeling, the lumped-parametrization for obtaining a relation between deformation of the finger-tip and its reproducing force is introduced. After that, a time-domain iterative learning control signal that eventually realizes desired trajectory tracking with satisfying a desired contact force is designed. Finally, some numerical simulations are performed and illustrated that it realizes desired trajectory tracking with satisfying a desired contact force.

II. A 5 D.O.F. ROBOTIC THUMB MODEL

A 5 D.O.F. robotic thumb model presented here has a soft and deformable hemispherical finger-tip as shown in Fig. 1. Assume that the finger-tip can only be rolling on a task plane, and it does not detach from the task plane during movements. The task plane is defined as the xy-plane in this paper. Any friction at each joint, or between the finger-tip and the task

This work was partially supported by "The Kyushu University Research Superstar Program (SSP)", based on the budget of Kyushu University allocated under President's initiative, and the Ministry of Education, Science, Sports and Culture, Grant-in-Aid for Young Scientists (B), 18760205, 2007.

K. Tahara is with the Organization for the Promotion of Advenced Research, Kyushu University, Fukuoka, 819-0395 JAPAN tahara@ieee.org

K. Tahara, S. Arimoto, M. Yoshida and Z.W. Luo are with the Bio-Mimetic Control Research Center, RIKEN, Nagoya, 463-0003 JAPAN yoshida@bmc.riken.jp

S. Arimoto and M. Sekimoto are with the Research Organization of Scinece and Engineering, Ritsumeikan University, Kusatsu, 525-8577 JAPAN {arimoto, sekimoto}@fc.ritsumei.ac.jp

Z.W. Luo is with the Department of Computer Science and Systems Engineering, Kobe University, Kobe, 657-8501 JAPAN luo@gold.kobe-u.ac.jp

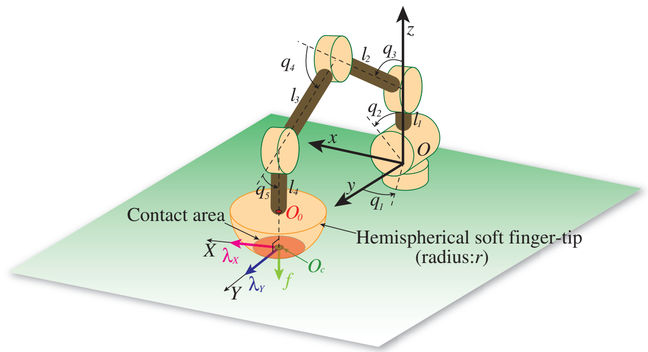

Fig. 1. A 5 D.O.F. robotic thumb model with soft and deformable hemispherical finger-tip

plane are omitted. In Fig. 1, symbol O is the center of the first and second joint (center of the saddle joint) of the robotic thumb and the origin of Cartesian coordinates. O_0 denotes the center of hemispherical soft finger-tip, and it can be expressed in Cartesian coordinates as $\boldsymbol{x_0} = (x_0, y_0, z_0)$, and O_c is the center of the contact area, and it can be expressed in Cartesian coordinates as $\boldsymbol{x_c} = (x_c, y_c, 0)$. Also the radius of hemispherical finger-tip is defined as a constant $r > 0$. Each joint angle $q_i(i{=}1{\sim}5)$ and each link length $l_j(j{=}1{\sim}4)$ are defined in Fig. 1.

A. 3-Dimensional Rolling Constraints

When a hemispherical finger-tip is purely rolling on the plane, a 3-Dimensional non-holonomic rolling constraints occur between the finger-tip and the task plane. Firstly, we introduce spherical polar local coordinates at the center of the finger-tip O_c as shown in Fig. 2. This spherical polar coordinates can be expressed by the vector of joint angle $\boldsymbol{q} = (q_1, q_2, q_3, q_4, q_5)^{\mathrm{T}} \in \mathbb{R}^5$ as follows:

$$\left[\begin{array}{l} \phi = \pi - q_3 - q_4 - q_5 \\ \eta = q_2 \end{array}\right. \tag{1}$$

Also the maximum displacement $\Delta z(t)$ of deformation at the center of the contact area on the finger-tip can be given

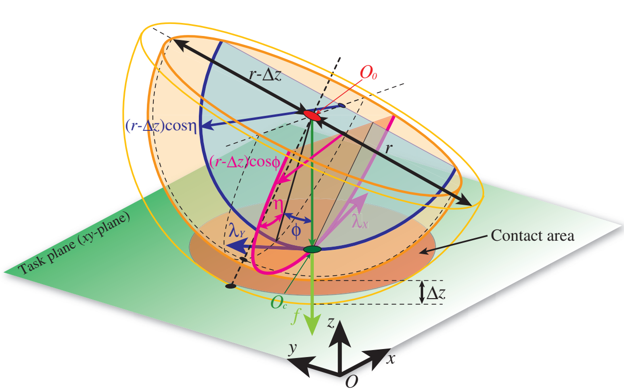

Fig. 2. Spherical polar local coordinates at the center of the finger-tip

as follows:

$$\Delta z(\boldsymbol{q}) = r - \cos q_2 \{l_1 + l_2 \cos q_3 + l_3 \cos(q_3 + q_4) + l_4 \cos(q_3 + q_4 + q_5)\} \tag{2}$$

In this model, the rotational movement of the finger-tip around the Z-axis at O_c (Spinning) can be ignored. It is well-known that the 3-Dimensional non-holonomic rolling constraints can be expressed such that the velocity of the center of the contact area on the hemispherical finger-tip expressed by the spherical polar local coordinates is equal to that on the task plane expressed by the joint coordinates [13]. Hence, the two non-holonomic rolling velocity constraints can be given as follows:

$$(r - \Delta z(\boldsymbol{q})) \frac{\mathrm{d}}{\mathrm{d}t} \{\cos\phi \cdot \eta\} + \frac{\mathrm{d}}{\mathrm{d}t}(Dq_1) = 0 \tag{3}$$

$$(r - \Delta z(\boldsymbol{q})) \frac{\mathrm{d}}{\mathrm{d}t} \{\cos\eta \cdot \phi\} + \frac{\mathrm{d}}{\mathrm{d}t} D = 0 \tag{4}$$

where $D = \sqrt{x_c^2 + y_c^2}$ stands for the distance between the center of the contact area O_c and the origin of Cartesian coordinates O. Equation (3) shows the rolling constraint toward X-axis at O_c, and eq. (4) shows the rolling constraint toward Y-axis at O_c. Equations (3) and (4) are linear and homogeneous with respect to the joint angular velocity vector $\dot{\boldsymbol{q}}$. Therefore, it can be reformulated as Pfaffian constraints in the following [13]:

$$\boldsymbol{A}\dot{\boldsymbol{q}} = 0 \tag{5}$$

where $\dot{\boldsymbol{q}} \in \mathbb{R}^5$ represents the angular velocity vector, and $\boldsymbol{A} \in \mathbb{R}^{2\times 5}$ represents the constraint matrix. It can be given as follows:

$$\boldsymbol{A} = \begin{pmatrix} (r - \Delta z(\boldsymbol{q})) \left(\cos\phi \dfrac{\partial \eta}{\partial \boldsymbol{q}} + \eta \dfrac{\partial(\cos\phi)}{\partial \boldsymbol{q}}\right)^{\mathrm{T}} \\ \qquad + \left(q_1 \dfrac{\partial D}{\partial \boldsymbol{q}} + D \dfrac{\partial q_1}{\partial \boldsymbol{q}}\right)^{\mathrm{T}} \\ (r - \Delta z(\boldsymbol{q})) \left(\cos\eta \dfrac{\partial \phi}{\partial \boldsymbol{q}} + \phi \dfrac{\partial(\cos\eta)}{\partial \boldsymbol{q}}\right)^{\mathrm{T}} + \dfrac{\partial D}{\partial \boldsymbol{q}}^{\mathrm{T}} \end{pmatrix} \tag{6}$$

Obviously, eq. (5) cannot be integrable in time t, and thereby this 3-Dimensional rolling constraints become non-holonomic.

B. Lumped-Parametrization for Modelling of Soft Finger-Tip

We introduce on the basis of lumped-parametrization a physical relation between deformation of the finger-tip material and its reproducing force. This parametrization method has been proposed by Arimoto *et al.* [14]. The reproducing force $f(\Delta z)$ in the normal direction to the task plane at the center of the contact area O_c is given as follows [14]:

$$\bar{f}(\Delta z) = k\Delta z^2 \tag{7}$$

where k is a positive stiffness constant which depends on the material of the finger-tip. It is reasonable to introduce a lamped-parametrized viscous force which depends on the material of the finger-tip. Therefore, the lumped-parametrized contact force equation is given as follows:

$$f(\Delta z, \Delta\dot{z}) = \bar{f}(\Delta z) + \xi(\Delta z)\Delta\dot{z} \tag{8}$$

In this model, $\xi(\Delta z)$ defined as a positive scalar function depending upon Δz. This viscous force is increasing with expansion of the contact area.

C. Dynamics of The Thumb Robot

By considering the elastic potential energy caused by deformation of the soft and hemispherical finger-tip, the total potential energy P and the total kinetic energy K of the robotic thumb model can be given as follows:

$$P = P_T(\boldsymbol{q}) + P_F(\Delta z) \tag{9}$$

$$K = \frac{1}{2}\dot{\boldsymbol{q}}^{\mathrm{T}}\boldsymbol{H}(\boldsymbol{q})\dot{\boldsymbol{q}} \tag{10}$$

where $\boldsymbol{H}(\boldsymbol{q}) \in \mathbb{R}^{5\times5}$ is the inertia matrix of the robotic thumb, $P_T(\boldsymbol{q})$ is the potential energy caused by the gravitational effect for the robotic thumb, and $P_F(\Delta z)$ is the elastic potential energy generated by deformation of the finger-tip and given by the following integration

$$P_F(\Delta z) = \int_0^{\Delta z} \bar{f}(\zeta)\mathrm{d}\zeta \tag{11}$$

Thus, Lagrangian L is given as:

$$L = K - P \tag{12}$$

and Hamilton's variational principle can be applied to Lagrangian L with considering the damping force on the finger-tip and the non-holonomic rolling constraint forces as external forces [15]. It is given as:

$$\int_{t_0}^{t_1}\left[\delta L + \boldsymbol{A}^{\mathrm{T}}\boldsymbol{\lambda} - \frac{1}{2}\frac{\partial\xi(\Delta z)\Delta\dot{z}^2}{\partial\Delta\dot{z}}\delta\Delta z + \boldsymbol{u}^{\mathrm{T}}\delta\boldsymbol{q}\right]\mathrm{d}t = 0 \tag{13}$$

where $\boldsymbol{\lambda} = (\lambda_X, \lambda_Y)^{\mathrm{T}} \in \mathbb{R}^2$ denotes the vector of Lagrange multipliers, and $\boldsymbol{u} \in \mathbb{R}^5$ is an input torque vector. Eventually, we obtain Lagrange's dynamic equation of motion in the following

$$\boldsymbol{H}(\boldsymbol{q})\ddot{\boldsymbol{q}} + \left\{\frac{1}{2}\dot{\boldsymbol{H}}(\boldsymbol{q}) + \boldsymbol{S}(\boldsymbol{q},\dot{\boldsymbol{q}})\right\}\dot{\boldsymbol{q}} - \boldsymbol{A}^{\mathrm{T}}\boldsymbol{\lambda} - \frac{\partial\Delta z}{\partial\boldsymbol{q}}^{\mathrm{T}} f + \boldsymbol{g}(\boldsymbol{q}) = \boldsymbol{u} \tag{14}$$

where $\boldsymbol{S}(\boldsymbol{q},\dot{\boldsymbol{q}}) \in \mathbb{R}^{5\times5}$ is a skew-symmetric matrix, and $\boldsymbol{g}(\boldsymbol{q}) \in \mathbb{R}^5$ is the gravitational term with respect to the potential energy $P_T(\boldsymbol{q})$. The physical meaning of $\boldsymbol{\lambda}$ is the rolling constraint forces. By taking inner product of the input $\boldsymbol{u}$ with the output $\dot{\boldsymbol{q}}$ and integrating it over time interval $t \in [0, T)$, we obtain

$$\int_0^t \dot{\boldsymbol{q}}^{\mathrm{T}}\boldsymbol{u}\,\mathrm{d}\tau = E(t) - E(0) + \int_0^t \xi(\Delta z(\tau))\Delta\dot{z}(\tau)^2\mathrm{d}\tau \leq -E(0) \tag{15}$$

where $E(t) = K + P$. This inequality shows that the input-output pair satisfies passivity [8].

III. ITERATIVE LEARNING CONTROL FOR SIMULTANEOUS FORCE/POSITION TRACKING TASKS

In this section, we introduce an iterative learning control signal to realize desired trajectory tracking of the center of the contact area $\boldsymbol{x_c}$ on the task plane with fulfilling a desired contact force f_d. In this paper, we assume that history data for the contact force f during a trial can be acquired by using force sensor to compose the iterative learning control signal for the contact force together with the contact position. The PI-type task space iterative learninig control signal is given as follows [4]

$$\boldsymbol{u}_n = -\boldsymbol{C}\dot{\boldsymbol{q}}_n - \boldsymbol{J_X}(\boldsymbol{q}_n)^{\mathrm{T}}\{\boldsymbol{K}\boldsymbol{\Delta x}_n - \boldsymbol{v}_n\} - \frac{\partial\Delta z}{\partial\boldsymbol{q}}^{\mathrm{T}}(f_d(t) - w_n) + \boldsymbol{g}(\boldsymbol{q}_n) \tag{16}$$

where symbol n stands for a trial number, $\boldsymbol{\Delta x}_n = (x_{0_n} - x_d(t),\ y_{0_n} - y_d(t))^{\mathrm{T}} \in \mathbb{R}^2$, $\boldsymbol{K} = \mathrm{diag}(k_x, k_y) \in \mathbb{R}^{2\times2}$, its componets k_x and k_y are positive constants, and r represents the radius of the finger-tip. $\boldsymbol{J_X}(\boldsymbol{q})^{\mathrm{T}} \in \mathbb{R}^{5\times2}$ signifies the Jacobian matrix for the x and y components of the center of finger-tip $\boldsymbol{x_0}$ with respect to $\boldsymbol{q}$, and $\boldsymbol{C} = \mathrm{diag}(c_1, c_2, c_3, c_4, c_5) \in \mathbb{R}^{5\times5}$ represents a damping matrix and each element $c_i (i = 1 \sim 5)$ is a positive constant. $\partial\Delta z/\partial\boldsymbol{q} \in \mathbb{R}^5$ is the Jacobian matrix for Δz with respect to $\boldsymbol{q}$ and it can be easily calculated from eq. (2) in real time. Also $\boldsymbol{g}(\boldsymbol{q}_n)$ stands for the gravity compensation term affecting the thumb, and $x_d(t)$, $y_d(t)$, and $f_d(t)$ are time-dependent desired contact position and force trajectories that lie on the task plane. The terms of $\boldsymbol{v}_n$ and w_n are feedforward position and force control signals generated by the iterative learning scheme, and are updated according to the following manner

$$\text{If} \quad n=1 \quad \begin{cases} \boldsymbol{v}_1 = 0 \\ w_1 = 0 \end{cases} \tag{17}$$

$$\text{If} \quad n>1 \quad \begin{cases} \boldsymbol{v}_n = \boldsymbol{v}_{n-1} - \{\boldsymbol{\Phi}\boldsymbol{\Delta}\dot{\boldsymbol{x}}_{n-1} + \boldsymbol{\Psi}\boldsymbol{\Delta x}_{n-1}\} \\ w_n = w_{n-1} + \Gamma\Delta f_{n-1} \end{cases} \tag{18}$$

where $\boldsymbol{\Phi} = \mathrm{diag}(\phi_x, \phi_y) \in \mathbb{R}^{2\times2}$ and $\boldsymbol{\Psi} = \mathrm{diag}(\psi_x, \psi_y) \in \mathbb{R}^{2\times2}$ denote P-gain and I-gain for the position learning respectivelly, and their compontes ϕ_x, ϕ_y, ψ_x, and ψ_y are positive constants. Also Γ denotes P-gain for the contact force learning, and $\Delta f_{n-1} = f_{n-1} - f_d$. It should be noted that the sensing information for the contact force f is used only in composing feedforward signal, and is not used in the feedback signal. Substituting eq. (16) into eq. (14) yields the closed-loop dynamics as follows:

$$\boldsymbol{H}(\boldsymbol{q}_n)\ddot{\boldsymbol{q}}_n + \left\{\frac{1}{2}\dot{\boldsymbol{H}}(\boldsymbol{q}_n) + \boldsymbol{S}(\boldsymbol{q}_n,\dot{\boldsymbol{q}}_n) + \boldsymbol{C}\right\}\dot{\boldsymbol{q}}_n - \boldsymbol{A}(\boldsymbol{q}_n)^{\mathrm{T}}\boldsymbol{\lambda}_n + \boldsymbol{J_X}(\boldsymbol{q}_n)^{\mathrm{T}}\boldsymbol{K}\boldsymbol{\Delta x}_n - \frac{\partial\Delta z_n}{\partial\boldsymbol{q}_n}^{\mathrm{T}}\Delta f_n = \boldsymbol{J_X}(\boldsymbol{q}_n)^{\mathrm{T}}\boldsymbol{v}_n + \frac{\partial\Delta z_n}{\partial\boldsymbol{q}_n}^{\mathrm{T}} w_n \tag{19}$$

In the next section, we will illustrate some results of numerical simulation to confirm that the position errors $\boldsymbol{\Delta x}_n$

TABLE I

PHYSICAL PARAMETERS OF THE ROBOTIC THUMB MODEL

Physical parameter	Value
1st link length l_1	0.01 [m]
2nd link length l_2	0.05 [m]
3rd link length l_3	0.03 [m]
4th link length l_4	0.02 [m]
1st link mass center l_{g_1}	0.05 [m]
2nd link mass center l_{g_2}	0.025 [m]
3rd link mass center l_{g_3}	0.015 [m]
4th link mass center l_{g_4}	0.01 [m]
1st link mass m_1	0.02 [kg]
2nd link mass m_2	0.02 [kg]
3rd link mass m_3	0.015 [kg]
4th link mass m_4	0.01 [kg]
1st link inertia I_1	$\mathrm{diag}(0.17, 0.17, 0.25)\times 10^{-6}$ [kg·m^2]
2nd link inertia I_2	$\mathrm{diag}(4.17, 4.17, 0.25)\times 10^{-6}$ [kg·m^2]
3rd link inertia I_3	$\mathrm{diag}(1.13, 1.13, 0.19)\times 10^{-6}$ [kg·m^2]
4th link inertia I_4	$\mathrm{diag}(0.33, 0.33, 0.13)\times 10^{-6}$ [kg·m^2]
Radius of finger tip r	0.01 [m]
Stiffness coefficient k	2.0×10^5 [N/m^2]
Damping scalar function ξ	$5.0 \times 10^4 \times (2r\Delta z - \Delta z^2)\pi$

TABLE II

DESIRED CONTACT FORCE, TERMINATION TIME, AND EACH GAIN

Parameter	Value
f_d	0.2 [N]
T	3.0 [sec]
$\boldsymbol{K}$	diag(10.0, 10.0)
$\boldsymbol{\Phi}$	diag(3.6, 3.6)
$\boldsymbol{\Psi}$	diag(1.5, 1.5)
Γ	1.0
$\boldsymbol{C}$	$\mathrm{diag}(10.0,\ 9.0,\ 2.0,\ 1.0,\ 0.5)\times 10^{-4}$

TABLE III

INITIAL CONDITION OF THE ROBOTIC THUMB MODEL

Variable	Value
$\boldsymbol{q}$	$(0.0,\ 0.0,\ 0.70,\ 1.59,\ 0.58)^{\mathrm{T}}$ [rad]
$(x_c,\ y_c)$	(0.0, 0.06) [m]
$f(\Delta z)$	0.2 [N]

and the force error Δf_n converge to zero while repeating the trial.

IV. NUMERICAL SIMULATION

Physical parameters of the 5 D.O.F. robotic thumb model such as masses and lengthes of the links used in the simulations are defined in Table I. In this paper, we set the time-dependent desierd trajectory on the task plane such that

$$\begin{pmatrix} x_d(t) \\ y_d(t) \end{pmatrix} = \begin{pmatrix} -0.002 + 0.002\cos\omega(t) \\ 0.060 + 0.002\sin\omega(t) \end{pmatrix} \tag{20}$$

where

$$\omega(t) = 2.0\pi \left\{ 6.0\left(\frac{t}{T}\right)^5 - 15.0\left(\frac{t}{T}\right)^4 + 10.0\left(\frac{t}{T}\right)^3 \right\} \tag{21}$$

and T represents a termination time for one trial. In addition, we choose the desired contact force f_d as a constant value. The desired contact force f_d, termination time T, feedback gain $\boldsymbol{K}$, learning gains $\boldsymbol{\Phi}$ and $\boldsymbol{\Psi}$, damping matirx $\boldsymbol{C}$ are defined as Table II. Initial position of the robotic thumb is given in Table III. The initial condition is used in all trial.

A. Results of Numerical Simulation

Figure 3 shows the transient responses for the contact force at the 1st to 10th trial. The contact force cannot follow the desired value, and the trajectory tracking error is quite large at the 1st trial, However at the 5th trial, the trajectory tracking error is decreased compared with that for the 1st trial. The desired contact force f_d is realized at the 10th trial. Figures 4 and 5 show the transient responses for x and y-component position of the center of the contact area at the 1st to 10th trial. At the 1st trial, the center of the contact area cannot follow the desired trajectory and the trajectory tracking errors are quite large. However at the 3th and 5th trials, the trajectory tracking errors are decreased compared with that for the 1st trial. The desired trajectories is realized at the 10th trial. The convergence performance for y-component is better than that for x-component. This result may come from the configuration of the thumb model that the number of joints to contribute to the motion of y direction is larger than that of x direction.

Figures 6 and 7 show the transient responses for the velocities of x and y-component of the center of the contact area at the 1st to 10th trial. As the same as the position of the center of the contact area, the velocity trajectory tracking at the 10th becomes faithful.

Figure 8 shows the position trajectories for the center of the contact area on the task plane. The trajectories of the center of the contact area converge to the desired one by repeating trials.

B. Simulation for Robustness

One of the benefits of the iterative learning control scheme is that accurate model information of the model is unnecessary in advance. In order to discuss the robustness of the control scheme, we perform another simulation with uncertain parameters. In previous simulations, we assume that the gravity term for the robotic thumb is well known in advance. However in the real world, we hardly get accurate model information about the robots. We assume that the gravity term is not accurate in the simulation, then we use an uncertain gravity compensation term in the input whose value is a half of actual values ($\tilde{\boldsymbol{g}}(\boldsymbol{q}) \approx \frac{1}{2}\boldsymbol{g}(\boldsymbol{q})$). Table IV shows the damping matirx $\boldsymbol{C}$ used in this simulation.

Figure 9 shows the transient responses of the contact force with uncertain gravity compensation term. At the 1st trial, actual contact force cannot trace the desired values. After

TABLE IV

DAMPING MATRIX FOR SIMULATION WITH UNCERTAIN GRAVITY TERM

$\boldsymbol{C}$	$\mathrm{diag}(15.0,\ 12.0,\ 10.0,\ 7.0,\ 3.0)\times 10^{-4}$

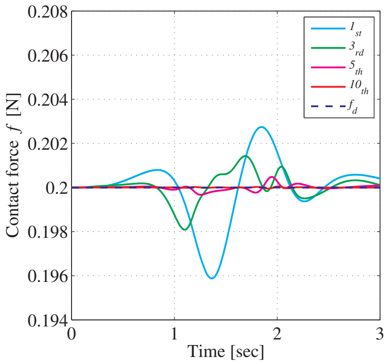

Fig. 3. Transient responses of the contact force induced by the deformation of the finger-tip

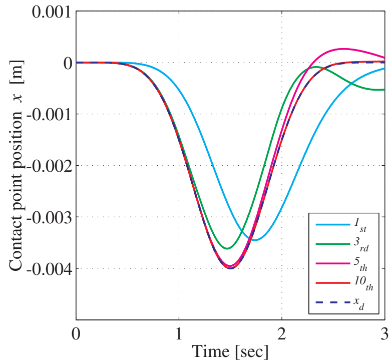

Fig. 4. Transient responses of x-component position of the center of the contact area

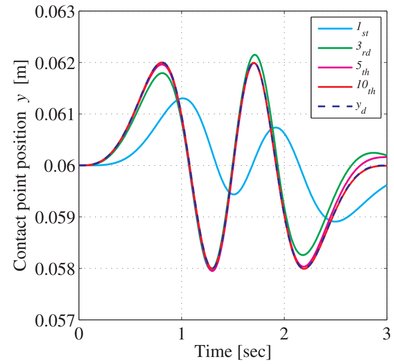

Fig. 5. Transient responses of y-component position of the center of the contact area

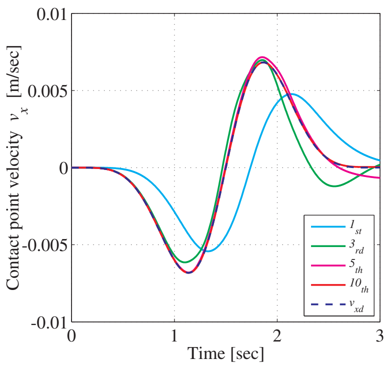

Fig. 6. Transient responses of x-component velocity of the center of the contact area

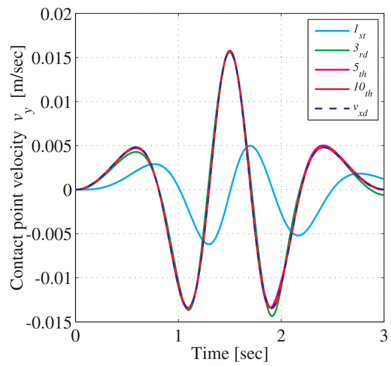

Fig. 7. Transient responses of y-component velocity of the center of the contact area

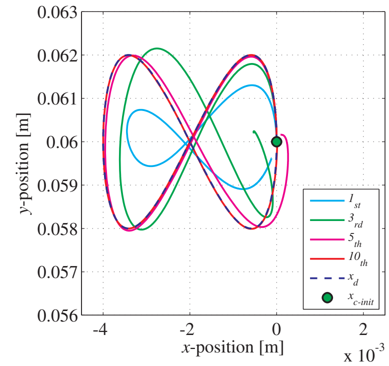

Fig. 8. Loci of the center of the contact area on the task plane

30^{th} trial, desired contact force is realized. At the beginning part of the 30^{th}, the small oscillation occurs. It might be caused by the initial error of the contact condition. Figures 10 and 11 show the transinent responses of x and y-component position of the center of the contact area. At the 1^{st} trial, both x and y-component trajectories are quite different from each desired value. However at the 30^{th} trial, both desired trajectories are realized. Figures 12 and 13 show the transient responses for the velocities of x and y-component of the center of the contact area. As the same as the position, both velocity trajectories are realized after 30^{th} trial. Figure 13 shows the position trajectories for the center of the contact area on the task plane. The trajectory of the 1^{st} trial is quite far from the desired one. After 30^{th} trial, the center of the contact area traces the desired one.

The robustness of this control method strongly depends on the values of the damping matrix $\boldsymbol{C}$. If $\boldsymbol{C}$ is too small, the robotic thumb cannot endure against the gravity effect, and even the 1^{st} trial cannot finish. In contrast, if the $\boldsymbol{C}$ is adequately large, this learning is sucsessfull even though the gravity compensation is not used. The learning speed also depends on the value of $\boldsymbol{C}$, that its speed becomes slower according to increasing of the value of $\boldsymbol{C}$. In this case, the learning speed can be improved by increasing the P-gain for the learning $\boldsymbol{\Phi}$.

From these simulation results, we can conclude that the iterative learning control for simultaneous force/position trajectory tracking is applicable and effective to reduce the trajectory tracking error on the task plane under non-holonomic rolling constraints, even though including some uncertain physical parameters for the robotic thumb model.

V. CONCLUTION

In this paper, we proposed an iterative learning control method for simultaneous force/position trajectory tracking tasks by using a 5 D.O.F. robotic thumb model under non-holonomic rolling constraints. Through some results of numerical simulations, we conclude that the trajectory tracking of position of the center of the contact area with fulfilling the desired contact force trajectory can be realized by using PI-type iterative learning control scheme. Moreover, the robustness for the learning method have demonstrated that even including some uncertain physical parameters for the robotic thumb, the learning can be performed. However, we have not yet treated convergency of the closed-loop dynamics and the trajectory tracking error while repeating trials, and the qualitative and quantitative evaluation for the robustness of this learning scheme analytically in this paper. In a future work, we must prove convergence of the trajectory tracking error rigorously, and analyze the robustness of this learning method in detail. Extensions of the proposed controller to more arbitrary situations would be more important. For

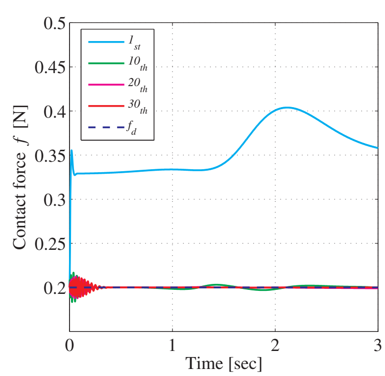

Fig. 9. Transient responses of the contact force with uncertain gravity compensation term

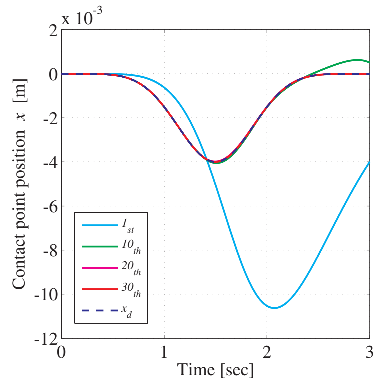

Fig. 10. Transient responses of x-component position of the center of the contact area with uncertain gravity compensation term

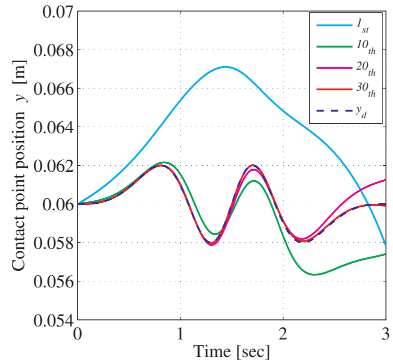

Fig. 11. Transient responses of y-component position of the center of the contact area with uncertain gravity compensation term

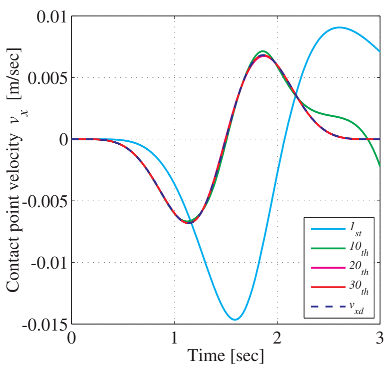

Fig. 12. Transient responses of x-component velocity of the center of the contact area with uncertain gravity compensation term

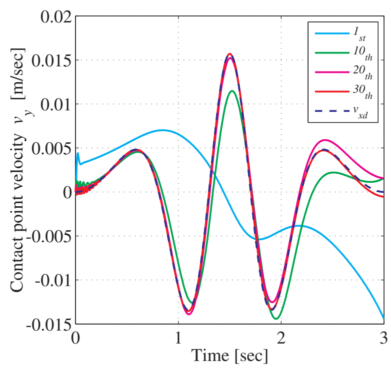

Fig. 13. Transient responses of y-component velocity of the center of the contact area with uncertain gravity compensation term

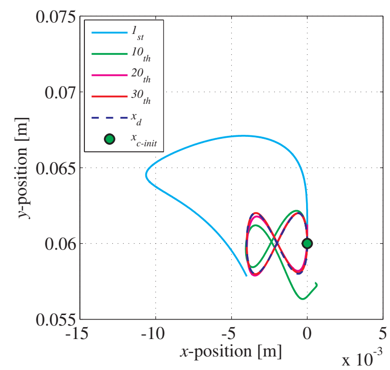

Fig. 14. Loci of the center of the contact area on the task plane with uncertain gravity compensation term

example, the task plane is not flat, or the shape of the finger-tip is not hemispherical. In parallel to these problems, we will develop an experimental setup and perform some experiments using a real 5 D.O.F. robotic thumb.

VI. ACKNOWLEDGMENTS

This work was partially supported by "The Kyushu University Research Superstar Program (SSP)", based on the budget of Kyushu University allocated under President's initiative, and the Ministry of Education, Science, Sports and Culture, Grant-in-Aid for Young Scientists (B), 18760205, 2007.

REFERENCES

[1] M. Uchiyama, "Formation of high-speed motion pattern of a mechanical arm by trial," *Trans. the Society of Instrumentation and Control Engineers*, Vol.14, pp.706-712, 1978. (in Japanese)

[2] S. Arimoto, S. Kawamura, and F. Miyazaki, "Bettering operation of robots by learning," *J. Robotic Systems*, Vol.1, No.2, pp.123-140, 1984.

[3] S. Kawamura, F. Miyazaki, and S. Arimoto, "Sensing of grasping condition by means of image processing," *Proc. the '85 Int. Conf. Advanced Robotics*, pp.235-242, Tokyo, Japan, 1985.

[4] S. Kawamura, F. Miyazaki, and S. Arimoto, "Realization of robot motion based on a learning method," *IEEE Trans. Systems, Man, and Cybernetics*, Vol.18, pp.126-134.

[5] T. Naniwa and S. Arimoto, "Learning control for robot tasks under geometric endpoint constraints," *IEEE Trans. Robotics and Automation*, Vol.11, pp.432-441, 1995.

[6] A. De Luca and F. Mataloni, "Learning control for redundant manipulators," *Proc. of the 1991 Int. Conf. Robotics and Automation*, pp.1442-1450, Sacrament, CA, 1991.

[7] A. De Luca, G. Paesano, and G. Ulivi, "A frequency-domain approachto learning control: implementation for a robot manipulator," *IEEE Trans. Industrial Electronics*, Vol.39, No.1, pp.1-10, 1992.

[8] S. Arimoto, *Control Theory of Non-linear Mechanical Systems – A Passivity-based and Circuit-theoretic Approach*, Oxford University Press, NY; 1996.

[9] S. Arimoto, M. Sekimoto, and S. Kawamura, "Iterative learning of specified motions in task-space for redundant multi-joint hand-arm robots," *Proc. the 2007 Int. Conf. Robotics and Automation*, Roma, Italy, 2007.

[10] K. Fujimoto, "On iterative learning control of nonholonomic Hamiltonian systems," *Proc. Mathematical Theory of Networks and Systems*, Leuven, Bergium, 2004.

[11] Y. Kiyasu, K. Fujimoto and T. Sugie, "Iterative learning control of nonholonomic Hamiltonian systems: Application to a vehicle system," *Proc. the 16th IFAC World Congress*, Prague, Czech Republic, 2005.

[12] K. Tahara, S. Arimoto, Z.W. Luo, and M. Yoshida, "On control for "blind touching" by human-like thumb robots," *Proc. the 2007 Int. Conf. Robotics and Automation*, Roma, Italy, 2007.

[13] R.M. Murray, Z. Li, and S.S. Sastry, *Mathematical Introduction to Robotic Manipulation*, CRC Press, Boca Raton; 1994.

[14] S. Arimoto, P.T.A. Nguyen, H.-Y. Han, and Z. Doulgeri, "Dynamics and control of a set of dual fingers with soft tips," *Robotica*, vol.18, no.1, 2000, pp.71-80.

[15] C. Lanczos, *The Variational Principles of Mechanics*, University of Toronto Press, Toronto; 1970.